

# *Saccharomyces cerevisiae* Nuclear and Nucleolar Antigen Preservation for Immunoelectron Microscopy

(*Saccharomyces cerevisiae* / nucleolus / nucleus / chemical fixation / high-pressure freezing / freeze-substitution / immunoelectron microscopy)

V. MISTRÍKOVÁ<sup>1</sup>, J. BEDNÁR<sup>1,2</sup>

<sup>1</sup>Charles University in Prague, First Faculty of Medicine, Institute of Cellular Biology and Pathology, and Institute of Physiology, Academy of Sciences of the Czech Republic, Department of Cell Biology, Prague, Czech Republic

<sup>2</sup>CNRS/UJF, Laboratoire de Spectrométrie Physique, UMR 5588, BP87, St. Martin d'Hères, France

**Abstract.** Yeast cells in general are known to be difficult to prepare for electron microscopy investigations particularly when the preservation of antigenicity is required. In this work, we compare various protocols for preparation of *Saccharomyces cerevisiae* cells for immunoelectron microscopy, ranging from classical chemical fixation to high-pressure freezing followed by freeze-substitution in different kinds of substitution media. Our aim was to establish a protocol giving optimal, routinely reproducible results for simultaneous retention of fine ultrastructural details and antigen immunoreactivity, with particular focus on the preservation of nuclear and nucleolar architecture. This was demonstrated by ultrastructural immunolocalization of various nucleolar (Nop1 and Nsr1), nuclear (Nsp1) and  $\alpha$ -tubulin antigens. The protocol which we found to yield the best preserved *Saccharomyces cerevisiae* cells for both morphological and immunological studies included cryo-fixation by high-pressure freezing fol-

lowed by freeze-substitution in acetone with 0.1% uranyl acetate and embedding in Lowicryl HM20. In addition, immunofluorescence detection of the antigens was performed and correlated with immunolabelling at the electron microscopy level.

## Introduction

The nucleolus is known to be a highly dynamic nuclear subcompartment where the processes of rRNA synthesis and ribosome biogenesis take place (Hernandez-Verdun, 2006; Sirri et al., 2008). Mostly, the nucleoli of higher eukaryotes are more or less spherical regions, often without direct contact with the nuclear envelope, varying greatly in size, number and structure according to the cell type and metabolic state. Classical transmission electron microscopy (TEM) permits one to distinguish three basic nucleolar subcompartments characterized by specific ultrastructural arrangement: the electron lucent fibrillar centres (FCs) surrounded by highly contrasted dense fibrillar components (DFCs) and the granular components (GCs) formed by pre-ribosomal particles (Mosgoeller, 2004; Shaw and Doonan, 2005; Sirri et al., 2008; Derenzini et al., 2009). Nucleoli of both budding (*Saccharomyces cerevisiae*) and fission (*Schizosaccharomyces pombe*) yeast are considerably smaller than those of higher eukaryotes and their organization into clearly distinguishable domains is less apparent. TEM micrographs of chemically fixed *S. cerevisiae* cells generally reveal the nucleolus as a dense, crescent-shaped region occupying up to one third of the nuclear volume, having extensive contacts with the nuclear envelope (Melese and Xue, 1995; Sicard et al., 1998; Trumtel et al., 2000). Especially in the case of yeast cells, chemical fixation appears to be insufficient to uncover the fine structural organization of the nucleolus. Moreover, its use strongly compromises the antigenicity of nuclear and nucleolar epitopes. Considerably better results can be achieved by low-temperature preparation and processing techniques (cryo-methods) that

Received October 27, 2009. Accepted January 26, 2010.

This work was supported by the Czech Grants Nos. MSM0021620806, LC535, AV0Z50110509, 303/03/H065 and 13308.

Corresponding author: Veronika Mistríková, Charles University in Prague, First Faculty of Medicine, Institute of Cellular Biology and Pathology, Albertov 4, 128 01 Prague 2, Czech Republic. Phone: (+420) 224 968 010; e-mail: vmist@lf1.cuni.cz

Abbreviations: BSA – bovine serum albumin, DFC – dense fibrillar component, DIC – differential interference contrast, EM – electron microscopy, ER – endoplasmic reticulum, FA – formaldehyde, FC – fibrillar centre, FS – freeze-substitution, GA – glutaraldehyde, GC – granular component, HPF – high-pressure freezing, IEM – immunoelectron microscopy, IF – immunofluorescence, KPi – potassium phosphate buffer, LM – light microscopy, NGS – normal goat serum, NPC – nuclear pore complex, PBS – phosphate-buffered saline, RT – room temperature, SPB – spindle pole body, TEM – transmission electron microscopy, UA – uranyl acetate, UV – ultraviolet light.

allow finer ultrastructural observations and improved immunocytochemical studies (Quintana, 1994). *S. cerevisiae* nucleolar subcompartments could only be distinguished in samples prepared in this way, though some morphological details (compared to higher eukaryotic cells) were still lost (Leger-Silvestre et al., 1999; Thiry and Lafontaine, 2005).

Nowadays, cryo-fixation by high-pressure freezing (HPF) followed by dehydration at subzero temperatures, i.e. freeze-substitution (FS), is the method of choice for the best preservation of cellular ultrastructure in numerous biological samples (e.g. Hawes et al., 2007; McDonald et al., 2007; Buser and Walther, 2008; Vanhecke et al., 2008). The cryo-preserved material displays an excellent morphology with considerably reduced numbers of artifacts when compared to chemically fixed samples. In this work, we apply these cryo-preparation methods to the study of the fine ultrastructure of *S. cerevisiae* nucleoli and to the immunolocalization of specific nuclear and nucleolar markers at the electron microscopy (EM) level. Although a number of protocols for chemical fixation (Wright, 2000; Mulholland and Botstein, 2002), cryo-fixation (Humbel et al., 2001; Walther and Ziegler, 2002; Giddings, 2003; McDonald et al., 2007; Murray, 2008) and Tokuyashu cryo-sectioning (Griffith et al., 2008) of yeast cells were proposed in the past, only a few have focused on fine nuclear and nucleolar antigen preservation in *S. cerevisiae* cells (Leger-Silvestre et al., 1999; Trumtel et al., 2000).

Here, we describe optimized recipes for *S. cerevisiae* preparation for immunoelectron microscopy (IEM) based on cryo-fixation by HPF followed by FS procedures and low-temperature embedding in Lowicryl HM20. Using these procedures, the cellular fine ultrastructure was retained to a great extent without loss of antigenicity. Their efficiency is demonstrated by direct comparison with equivalent immunolabelling experiments performed on conventionally chemically fixed and LR White-embedded *S. cerevisiae* cells. Our results show that the immunoreactivity of two proteins that were analysed (Nsr1 and Nsp1) was preserved exclusively in cryo-processed cells. Simultaneously, immunofluorescent visualization of the target antigens was performed at the light microscopy (LM) level.

## Material and Methods

### *Yeast strain, media and cultivation conditions*

The *S. cerevisiae* haploid strain NOY 886 (*MATa rpa135Δ::LEU2 ade 2-1 ura3-1 his 3-11 trp1-1 leu2-3,112 can1-100 fob1Δ::HIS3* pNOY117 [*CEN RPA135 TRP1*]) (a kind gift of Yvonne S. Osheim, University of Virginia Health System, Charlottesville, VA) was used throughout this study. Cells were grown at 26 °C in a standard YPD medium containing 1 % yeast extract, 2 % peptone, 2 % D-(+)-glucose and 100 µg/ml adenine hemisulphate salt.

Unsynchronized yeast cells were used in each experiment. The day prior to fixation, a single colony of the yeast cells was used to inoculate 100 ml of YPD medium in a 250-ml Erlenmeyer flask and grown overnight with moderate shaking. The next day, the overnight culture was used to inoculate 5 ml of fresh YPD medium and grown to an early log phase (OD 600 0.2–0.4, corresponding to less than 10<sup>7</sup> cells/ml), then processed for the LM or EM studies.

### ***Preparation of S. cerevisiae cells for immunoelectron microscopy***

#### *High-pressure freezing*

Cryo-fixation was performed using a Leica EM PACT2 high-pressure freezer equipped with a rapid transfer system (Leica Microsystems, Vienna, Austria) as described previously (McDonald and Müller-Reichert, 2002). Approximately 5-ml aliquots of yeast culture (OD 0.2–0.4) were harvested by vacuum filtration using a 15-ml suction filtration apparatus (Millipore, Billerica, MA) on 0.45-µm nitrocellulose membrane filters (Macherey Nagel, Düren, Germany), then placed on a plate with 1% agar in YPD medium in order to prevent dehydration of the yeast during the transfer. Using a sterile toothpick, the yeast paste was scraped off the filter onto a membrane carrier (1.5 mm in diameter, 0.1 mm deep, Cat.# 16707898, Leica instruments, Vienna, Austria) under a stereomicroscope. Precautions were taken to thoroughly fill the entire volume of the carrier cavity. The samples were immediately high-pressure frozen (HP-frozen) and stored under liquid N<sub>2</sub> until FS. The time interval between the harvesting of the cells and freezing was kept under one minute.

#### *Freeze-substitution*

Freeze-substitution was performed using an automatic FS instrument (Leica EM AFS2, Leica Microsystems) equipped with an EM FS processor. HP-frozen samples were first placed into a reagent bath loaded with one of the FS solutions under test pre-cooled to -90 °C, and processed for 24 h. Next, the temperature was gradually increased at a rate of 5 °C/h (8 h in total) to -50 °C and held constant for 24 h. All successive processing steps were performed at this temperature. Samples were then washed three times with pure acetone and gradually infiltrated with 3 : 1, 1 : 1 and 1 : 3 acetone : resin (v : v) mixtures, 2 to 3 h for each step. Lowicryl HM20 (HM20 kit, Cat.# 14340, Electron Microscopy Sciences, Hatfield, PA) was used for low-temperature embedding. Before use, the resin was degassed with a stream of dry N<sub>2</sub> to remove oxygen, which could interfere with the polymerization. The mixture was exchanged with pure resin at least three times, using 2 h for each incubation. Polymerization under UV light (using a UV LED lamp integrated in the FS processor) was performed for 24 h at -50 °C and for an additional 24 h at +20 °C (the temperature was gradually increased at a rate of 5 °C/h – 14 h in total).

The following FS media were used: (1) anhydrous acetone (EM grade, Polysciences Europe GmbH, Eppelheim, Germany); (2) acetone with 0.1% glutaraldehyde (GA) – made from a 50% aqueous GA stock solution (Electron Microscopy Sciences); (3) acetone with 0.1% uranyl acetate (UA, Merck, Darmstadt, Germany) – prepared from a 10% methanolic stock solution a day prior to the experiment, then filtered three times through a syringe filter (0.22  $\mu\text{m}$ ) before use, and (4) acetone with 0.1% UA and 0.1% GA.

### *Chemical fixation*

Yeast cells were fixed in a solution of 4% (w/v) formaldehyde (FA, Fluka, Buchs, Switzerland) in 0.1 M PIPES (pH 6.8), 1 mM  $\text{CaCl}_2$ , 1 mM  $\text{MgCl}_2$  and 0.1 M D-sorbitol with or without addition of various concentrations of GA (0.05 to 0.5%) for 1 h at room temperature (RT). The cells were washed twice, for 15 min, in 0.1 M PIPES with 0.1 M D-sorbitol and once in 0.1 M PIPES alone and treated with 1%  $\text{NaIO}_4$  and 50 mM  $\text{NH}_4\text{Cl}$  as described (Mulholland and Botstein, 2002). Dehydration was performed successively on ice in graded ethanol series (25, 50, 75, 95 and 100% ethanol) in 5-min steps. Three changes of 100% ethanol were applied and the final step was performed at RT. The dehydrated cells were infiltrated with 2 : 1, 1 : 1 and 1 : 2 ethanol : LR White resin (v : v) mixtures and twice with pure LR White (Medium grade, kit, Cat.# 14380, Electron Microscopy Sciences), each step was for 1 h at RT. The third infiltration step was performed overnight at 4 °C. The next day, the resin was again exchanged, and incubated for about 30 min at RT. Finally, the samples were transferred into gelatin capsules (size 1, Leica instruments) containing fresh resin, allowed to settle for 15 min and polymerized at 47 °C for 2 or 3 days.

### *Microtomy, staining and electron microscopy*

Ultrathin sections (60 nm) were prepared in a Reichert Ultracut S microtome using a diamond knife (45° Diatome, Ft. Washington, PA) and collected on Formvar/carbon-coated nickel or copper grids. Sections of chemically fixed yeast cells were post-stained using 2% aqueous uranyl acetate for 5 min and lead citrate (Reynolds, 1963) for 1 min. Sections of HP-frozen/acetone alone or acetone/GA-substituted cells were post-stained similarly as described above, except that 2% uranyl acetate in 70% methanol was used. Sections of acetone/UA or acetone/UA/GA-substituted cells were not post-stained. The samples were then imaged with a Tecnai G2 Sphera transmission electron microscope (FEI Company, Brno, Czech Republic) operating at 120 kV. Images were recorded with a Gatan Ultrascan 1000 CCD camera (Gatan Inc., Warrendale, PA).

### *Immunolabelling*

Thin sections mounted on nickel grids were first pre-blocked with 5% (w/v) normal goat serum (NGS) in phosphate-buffered saline (PBS, pH 7.4) for 30 min and then incubated with primary antibody diluted in 1%

(w/v) bovine serum albumin (BSA) and 0.05% Tween-20 in PBS for 1 h and 45 min in a humid chamber at RT. Afterwards, the grids were first washed in 0.05% Tween-20 in PBS and then in PBS alone. Before the secondary antibody was applied, the grids were blocked with 1% NGS in PBS for 10 min. Gold-conjugated secondary antibody was diluted in PBS and incubation was performed for 1 h in a humid chamber at RT. Finally, the grids were washed in PBS and in double-distilled water, air-dried, and post-stained as described above or, alternatively, left unstained. In negative control experiments the incubation with primary antibody was omitted.

For quantification of immunogold labelling, Nop1 and Nsr1 antigens were selected according to their specific localization in the nucleolus. Sets of 10 micrographs of yeast cell nuclei (nucleoli) at a magnification of x 7800 were chosen randomly for each of the FS media and labelling density was determined in terms of a number of gold particles per square micrometer. For each set, an average and standard deviation were determined. The density was evaluated for the nucleolus and for the rest of the cell section, giving thus the information about the level of non-specific labelling. The measurements were performed using ImageJ software (Rasband, W. S., ImageJ, U. S. National Institutes of Health, Bethesda, Maryland, USA, <http://rsb.info.nih.gov/ij/>, 1997-2009).

### *Immunofluorescence microscopy*

The cells were fixed with 4% (w/v) FA in 0.1 M potassium phosphate buffer (KPi), pH 6.8, added directly to the growing culture as a 2x stock. Fixation was performed for 2 h at RT. Fixed cells were washed twice in 0.1 M KPi and once in 0.1 M KPi with 1.2 M D-sorbitol (solution P). Cell walls were removed using zymolyase (Cat.# E1004, ZymoResearch, Orange, CA) diluted 1 : 50 in solution P at 30 °C for 10 to 20 min. Digestion of the cell walls was monitored by phase-contrast light microscopy using a 100x oil-immersion objective. The spheroplasted cells were washed again in solution P and left to sediment for 10 min on poly-L-lysine (0.01% solution, Sigma, Saint Louis, MO) treated coverslips. Permeabilization of the cells was performed as described by Pringle et al. (1989) with 0.1% Triton X-100 in PBS for 30 min at RT or alternatively by dipping the coverslips into methanol for 6 min and subsequently into acetone for 30 s, both at -20 °C. Next, the samples were pre-blocked for 20 min with the blocking buffer (1% (w/v) BSA in PBS, pH 7.4), incubated for 1 h with primary antibody, washed in PBS and incubated for an additional 1 h with fluorescent secondary antibody. Both antibodies were diluted in the blocking buffer and all steps were performed at RT. Finally, the cells were washed in PBS and in double-distilled water, embedded in Mowiol/DABCO mounting medium (Fluka) containing 0.4  $\mu\text{g}/\text{ml}$  DAPI and placed onto slides. The cells were examined with a Leica TCS SP5 laser scanning confocal microscope (Leica Microsystems) using a 100x/1.4 NA oil-immersion objective.

## Antibodies

The following primary antibodies were used: (a) anti-fibrillarin (Abcam plc, Cambridge, UK), diluted 1 : 500 for LM and 1 : 5 for EM; (b) anti-Nsr1p (Abcam), diluted 1 : 400 for LM and 1 : 7 for EM; (c) anti-Nsp1p (Abcam), diluted 1 : 450 for LM and 1 : 5 for EM and (d) anti- $\alpha$ -tubulin (Sigma) diluted 1 : 2000 for LM and 1 : 50 for EM. All used primary antibodies were mouse monoclonal, IgG isotype. Cy3-labelled donkey anti-mouse secondary antibody diluted 1 : 500 and 12 nm gold conjugated goat anti-mouse secondary antibody diluted 1 : 10 (both from Jackson ImmunoResearch, Suffolk, UK) were used for LM and EM detection, respectively.

## Results

### Chemically fixed cells

#### Formaldehyde-fixed cells

Typically, 4% FA-fixed cells (Fig. 1A) exhibited irregular shapes and most of the cellular organelles showed improper preservation. The cytoplasm was retracted and distinct plasma membrane invaginations into the cytoplasm were observed frequently (black arrows). The vacuoles were rather small and numerous in most cases, and their contents were almost always lost. The mito-

chondria, Golgi cisternae, endoplasmic reticulum (ER) and nucleus were distinguishable only thanks to the white profile of their membranes, very likely a consequence of omitting  $\text{KMnO}_4$  and/or  $\text{OsO}_4$  treatment (Wright, 2000). Prominently, the shape of the nuclear envelope was strongly irregular and nuclear organization, i.e. the presence of recognizable regions of heterochromatin and euchromatin, was almost invisible. In the majority of the nucleoli that were investigated, the FC/DFC/GC compartments were not recognizable, though zones of lower and higher electron densities were observed.

#### Formaldehyde/Glutaraldehyde-fixed cells

The ultrastructural preservation in FA/GA-fixed cells was apparently better (Fig. 1B-D) despite the fact that the GA concentrations that were used were kept low (from 0.05 to 0.5 %) due to the requirement of antigenicity preservation. Generally, the cytoplasmic organelles showed morphology similar to that of FA-fixed cells, and plasma membrane invaginations were still present (black arrows); however, the retractions of the cytoplasm were nearly eliminated. Preservation of the vacuolar content gradually improved with increasing concentration of GA, though without reaching an acceptable level. Nuclear shape was still strongly irregular and the nucleoplasm showed a homogeneous grainy texture. As in FA-fixed cells, the nucleolar subcompartments were hardly recognizable.

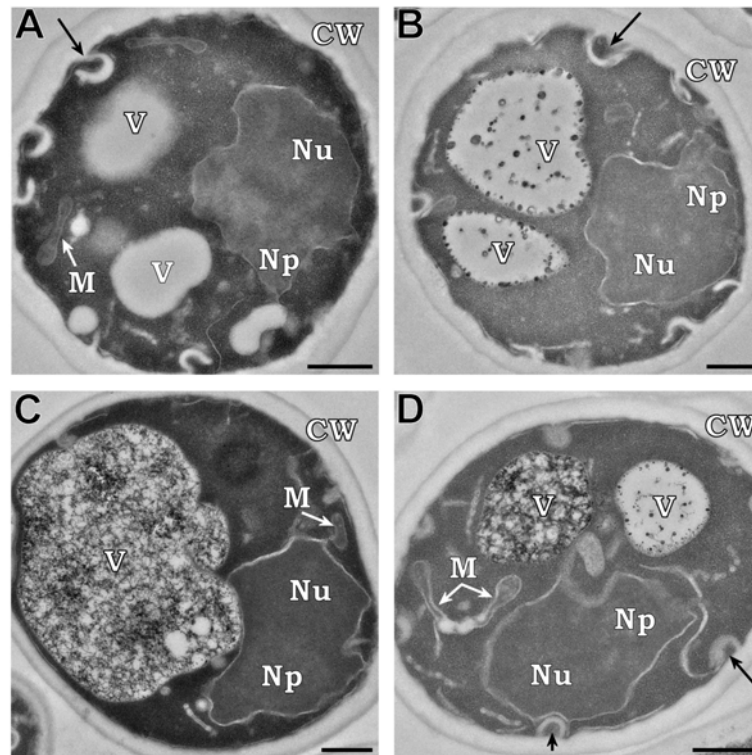


Fig. 1. Morphology of chemically fixed and LR White-embedded *S. cerevisiae* cells. Conventional fixation for TEM (IEM) with A – 4% FA alone, B – 4% FA in combination with 0.05% GA, C – with 0.3% GA, and D – with 0.5% GA. Black arrows point to plasma membrane invaginations. CW, cell wall; M, mitochondria; Np, nucleoplasm; Nu, nucleolus; V, vacuole. Sections were post-stained. Scale bar = 500 nm.

### High-pressure freezing and freeze-substitution

We next performed cryo-fixation by the HPF method and subsequently processed *S. cerevisiae* cells at low temperatures by the FS procedure using various substitution solutions (see Material and Methods). Low-viscosity non-polar Lowicryl HM20 was selected as an embedding medium as it permits processing of samples at subzero temperatures and has been used successfully for IEM procedures (van Tuinen and Riezman, 1987; Hofmann et al., 1998; Giddings, 2003).

#### FS medium 1: acetone alone

The substitution of *S. cerevisiae* cells in acetone alone (Fig. 2A) resulted in structural and ultrastructural preservation noticeably superior to that generally observed in aldehyde-fixed cells (Fig. 1). Lowicryl HM20 (and K4M) is known to produce high contrast of the sections compared to other embedding media (Bendayan and Shore, 1982). Thus, even in unstained sections (data not shown) the major morphological features of the cells (e.g. vacuoles, nuclei) were obvious, but finer details were difficult to distinguish unless the post-staining procedure was applied (Fig. 2A). The overall ultrastructural preservation of the cells was very good, though infiltration with the resin was imperfect in many cases. Gaps between the resin and the cells were commonly observed. In some cases, whole cells popped out of the sections (data not shown).

#### FS medium 2: acetone with 0.1% glutaraldehyde

The cells substituted in acetone with 0.1% GA (Fig. 2B) showed better resin infiltration (no yeast cells were lost during the preparation of thin sections) and ultrastructural preservation was similar to that observed in acetone-only substituted yeast cells. As revealed by post-staining, all cytoplasmic structures in the cells (mitochondria, ERs, Golgi compartments, nuclei, etc.) were well preserved.

#### FS medium 3: acetone with 0.1% uranyl acetate

The best results were obtained with substitution in acetone with 0.1% UA (Fig. 2C). Even at this concentration of UA, the overall contrast of the sections was notably enhanced, in accordance with previous observations (Walther and Ziegler, 2002; van Donselaar et al., 2007). Moreover, fine contours of the membranes were emphasized, thus the individual organelles were readily recognized even without the use of the post-staining procedure.

#### FS medium 4: acetone with 0.1% uranyl acetate and 0.1% glutaraldehyde

The results obtained when acetone containing both 0.1% UA and 0.1% GA (Fig. 2D, 3A) was used were very similar to those of acetone/GA-substituted sam-

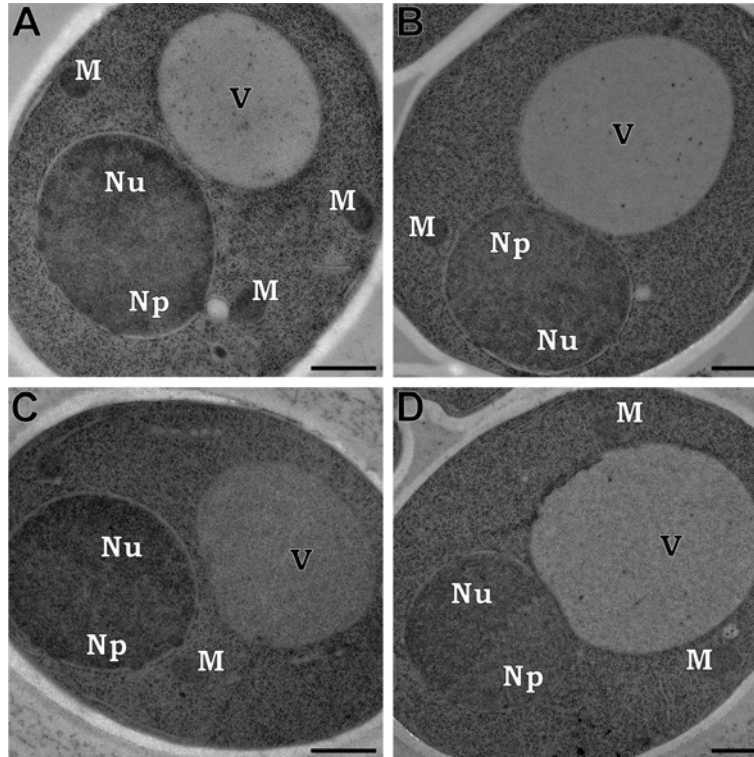
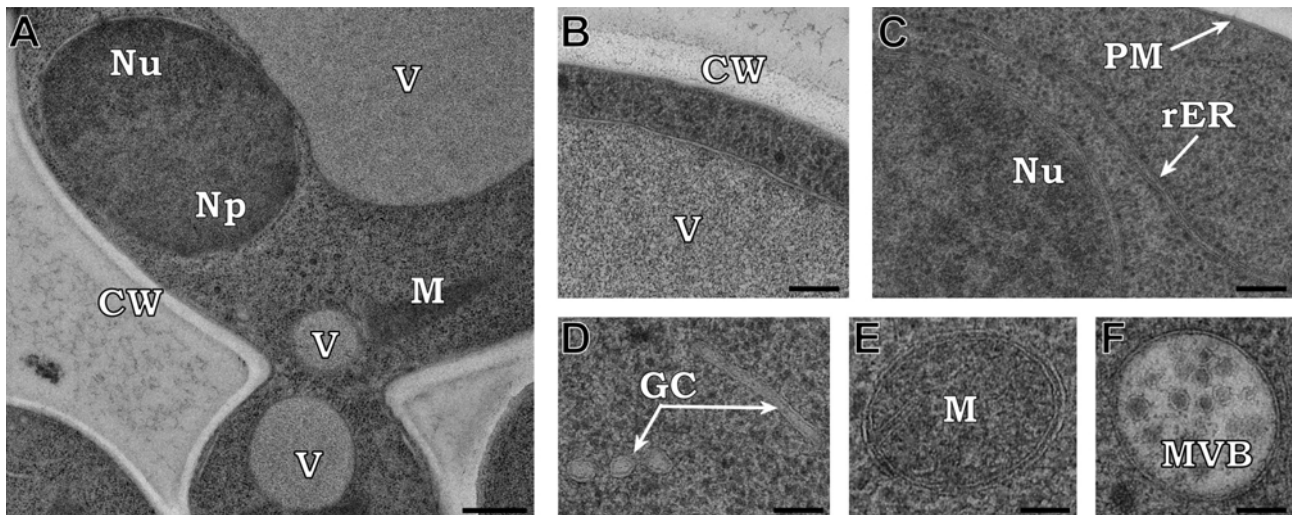


Fig. 2. Morphology of Lowicryl HM20-embedded *S. cerevisiae* cells after high-pressure freezing and freeze-substitution in different media. Substitution in A – acetone alone, B – acetone with 0.1% GA, C – acetone with 0.1% UA, and D – acetone with 0.1% UA + 0.1% GA. M, mitochondria; Np, nucleoplasm; Nu, nucleolus; V, vacuole. Sections were post-stained (A, B) or left without post-staining (C, D). Scale bar = 500 nm.



**Fig. 3.** Details of various cell components preserved in *S. cerevisiae* cells after high-pressure freezing and freeze-substitution. A – budding yeast cell substituted in acetone with 0.1% UA + 0.1% GA. B–F – fine ultrastructural details of the cells substituted in acetone with 0.1% UA. CW, cell wall; GC, Golgi cisternae; NE, nuclear envelope; Np, nucleoplasm; Nu, nucleolus; M, mitochondria; MVB, multivesicular body; PM, plasma membrane; rER, rough endoplasmic reticulum; V, vacuole. Sections were not post-stained. Scale bar = 500 nm (A), 200 nm (B, C, E, F) and 100 nm (D).

ples. The quality of the structure preservation was the same, though the contrast was significantly better.

Overall, all the FS media that were used yielded well-preserved *S. cerevisiae* cells compared to conventionally aldehyde-fixed cells (compare Fig. 1 and Fig. 2). As shown in Fig. 3, the cell walls, plasma membranes, vacuolar membranes, nuclear envelopes, etc. showed smooth and continuous contours. Moreover, the fine details of the cell walls were very well preserved in a great majority of the cells (Fig. 3B). Plasma membrane invaginations were less pronounced. The vacuoles had spherical shapes and contents of uniform density (Fig. 3A, B). In the cytoplasm, the individual ribosomes, rough ER (Fig. 3C), Golgi cisternae (Fig. 3D), mitochondria (Fig. 3E), multivesicular bodies (Fig. 3F), etc. were clearly distinguishable. Regular and smooth profiles of the nuclei were always observed (Fig. 3A and 4A). When UA was added to the FS solution, it was much easier to observe the double membrane profile of the nuclear envelope (Figs. 3C, 4A, B) and its interruption by nuclear pores (Fig. 4A, B, arrowheads) than it was in acetone-only or acetone/GA-substituted yeast cells.

Microtubules (Fig. 4C) and spindle pole bodies (SPB) were also easily localized (Fig. 4D, E). Generally, substitution with acetone/UA FS medium yielded the best overall results, but some particular structures, e.g. SPB mentioned above (compare Fig. 4D and 4E), were better defined when the stain was not present in the FS medium and their contrast was obtained by post-staining. The nuclear and nucleolar chromatin was always well preserved and very dense in all four types of FS media described above (Fig. 5A–D). In the nucleolar region, FCs were easily distinguished as the zones of lower electron densities (Fig. 5, asterisks) surrounded by elec-

tron-dense areas in which both dense fibrils and pre-ribosomal particles were localized (arrowheads).

#### *Immunofluorescence and immunoelectron microscopy*

Next, the ultrastructural immunolocalization of various antigens related to nuclear and nucleolar function was examined on thin sections of both chemically fixed (data not shown) and HP-frozen/FS *S. cerevisiae* cells. Nop1 and Nsr1 were used as nucleolar markers, Nsp1 as a nuclear envelope marker and  $\alpha$ -tubulin as a marker of microtubules. Each of the proteins that were analysed was first specifically localized via indirect immunofluorescent (IF) staining of permeabilized yeast cells.

#### *Nop1 protein*

Nop1 is a yeast nucleolar protein known to be structurally and functionally homologous to vertebrate fibrillar, which is essential for viability and pre-rRNA processing (Schimmang et al., 1989; Tollervey et al., 1991). Nop1 was previously specifically localized both by indirect IF (Schimmang et al., 1989; Tollervey et al., 1991; Qiu et al., 2008) and IEM procedures (Leger-Silvestre et al., 1999; Trumtel et al., 2000). As expected, our experiments revealed a specific, intense and often crescent-shaped labelling pattern characteristic of the yeast nucleolus at the LM level (Fig. 6A). Consistent with IF results, Nop1 was localized to the nucleolus at the EM level, predominantly to the dense areas surrounding the FCs of lower electron densities (Fig. 6B, arrowheads). The pattern of labelling was similar in both chemically fixed and cryo-processed cells; however, the intensity of the labelling and localization with respect to the individual nucleolar subcompartments was more prominent on sections of HP-frozen/FS yeast cells.

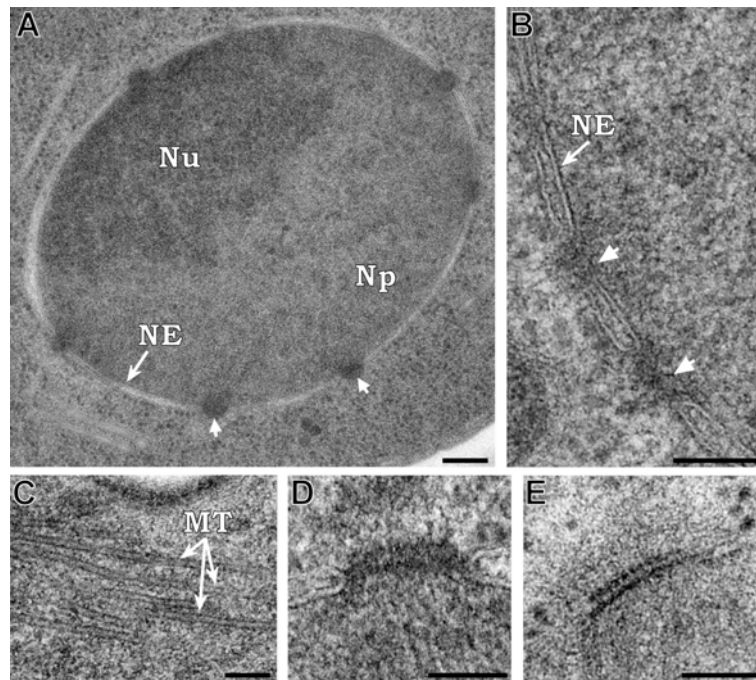


*Fig. 4.* Details of selected nuclear structures demonstrating fine ultrastructure preservation obtained by high-pressure freezing and freeze-substitution of *S. cerevisiae* cells, embedded in Lowicryl HM20. A – overview of the nucleus. B – nuclear pores (arrowheads) embedded in the nuclear envelope. C – microtubules (arrows) in longitudinal section. D, E – a single spindle pole body. MT, microtubules; NE, nuclear envelope; Np, nucleoplasm; Nu, nucleolus. The cells were substituted either in acetone with 0.1% UA and sections left without post-staining (A–D) or in acetone with 0.1% GA and post-stained (E). Scale bar = 200 nm (A), 100 nm (B–E).

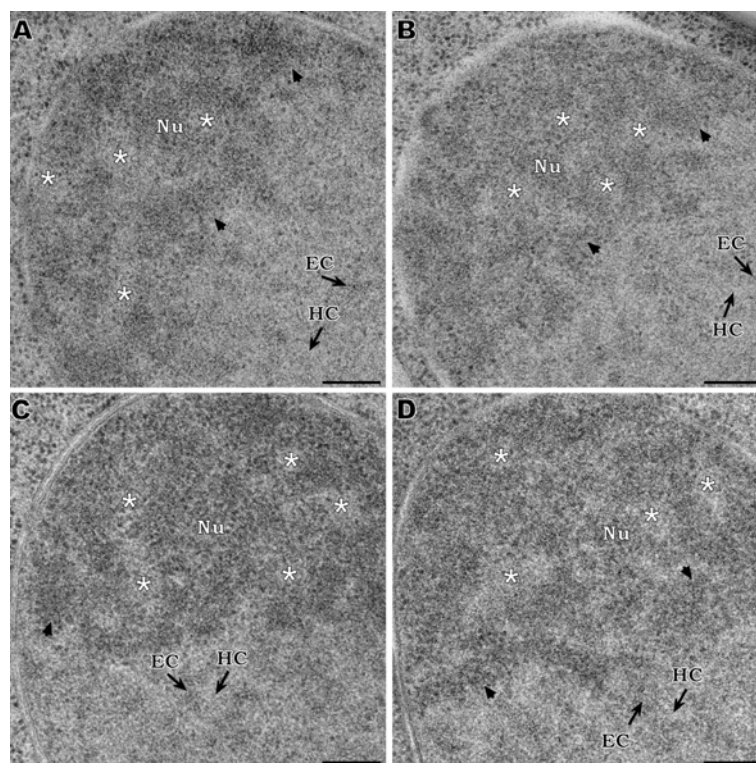


*Fig. 5.* Nucleolar ultrastructure preservation of high-pressure frozen *S. cerevisiae* cells substituted in different media. The nuclei of the cells substituted in A – acetone alone, B – acetone with 0.1% GA, C – acetone with 0.1% UA, and D – acetone with 0.1% UA + 0.1% GA. Fibrillar centres are marked by asterisks, dense fibrillar and granular areas by arrowheads. HC, heterochromatin; EC, euchromatin; Nu, nucleolus. Sections were post-stained (A, B) or left without post-staining (C, D). Scale bar = 200 nm.

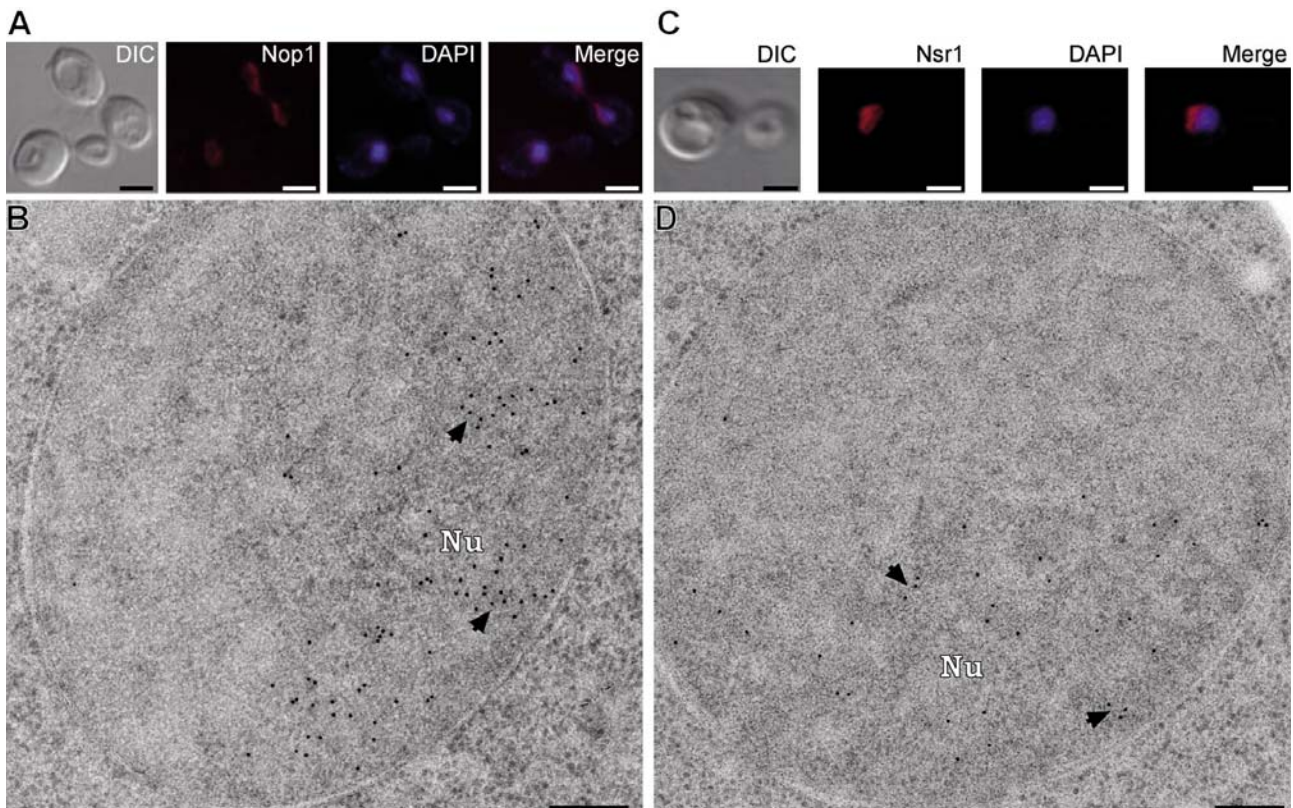


**Fig. 6.** Comparative immunolocalization of the nucleolar markers Nop1 and Nsr1 in *S. cerevisiae* cells at the LM and EM levels. A, C – differential interference contrast (DIC), indirect immunofluorescent localization of Nop1 and Nsr1, respectively (red), nuclear DNA staining with DAPI (blue) and their merge. The primary antibodies were visualized with a Cy3-conjugated secondary antibody. B, D – post-embedding on-section immunogold (12 nm) labelling of Nop1 and Nsr1, respectively, at the EM level (arrowheads). Nu, nucleolus. *S. cerevisiae* cells were freeze-substituted in acetone with 0.1% UA and embedded in Lowicryl HM20. Sections were not post-stained. Scale bar = 3  $\mu$ m (A, C), 100 nm (B), 200 nm (D).

### *Nsr1* protein

Nsr1 is a non-ribosomal nucleolar protein known as the vertebrate nucleolin orthologue (Lee et al., 1992; Yan and Melese, 1993) and functional homologue of *Schizosaccharomyces pombe* gar2 protein (Gulli et al., 1995). Similarly to Nop1, Nsr1 is involved in rRNA maturation, ribosome assembly and possibly in nucleocytoplasmic transport (Kondo and Inouye, 1992; Lee et al., 1992; Gulli et al., 1995). In agreement with previous results (Yan and Melese, 1993; Xu et al., 2003), we have specifically localized Nsr1 to the *S. cerevisiae* nucleolus using indirect IF staining (Fig. 6C). As reported earlier (Leger-Silvestre et al., 1997), *S. pombe* gar2 protein was localized at the EM level along the DFCs and around the FCs, although nucleolin was detected in DFCs and rarely in both the GCs and FCs in vertebrate cells (Spector et al., 1984; Escande et al., 1985). However, the immunocytochemical detection of *S. cerevisiae* Nsr1 protein has not been reported. Here, thin sections of HP-frozen/FS and chemically fixed yeast cells were used for Nsr1 localization using on-section immunogold labelling. Gold particles were mainly distributed along and/or in the dense parts of the nucleolus, in agreement with Leger-Silvestre et al. (1997) results. Importantly, no labelling was detected on thin sections of chemically fixed yeast cells.

### *Nsp1* protein

Nsp1 is one of the most abundant nucleoporins in the yeast. It plays an important role in facilitating bidirectional transport of materials through nuclear pore complexes (NPC) (Fahrenkrog et al., 2000; Bailer et al., 2001). Previously, Nsp1 was specifically localized by a pre-embedding method at the EM level (Fahrenkrog et al., 2000). Here, indirect IF staining of Nsp1 revealed the *S. cerevisiae* nuclear envelope (Fig. 7A). Next, we immunolocalized Nsp1 on thin sections of both chemically fixed and HP-frozen/FS *S. cerevisiae* cells. Consistent with previous results, most of the NPCs present in the sections of HP-frozen/FS yeast cells were specifically labelled. The gold particles were detected inside the NPCs and both on their nucleoplasmic and cytoplasmic sides (Fig. 7B, arrowheads). No Nsp1 signal was detected on sections of chemically fixed cells.

### $\alpha$ -Tubulin

Immunodetection of  $\alpha$ -tubulin in *S. cerevisiae* cells is shown in Fig. 8A, B. Microtubules running from the SPBs embedded in the nuclear envelope were specifically labelled both by indirect IF staining (Fig. 8A) and by on-section immunogold labelling (Fig. 8B). Both patterns were consistent with previous results (Kilmartin and Adams, 1984; Sato et al., 1996; Müller-Reichert

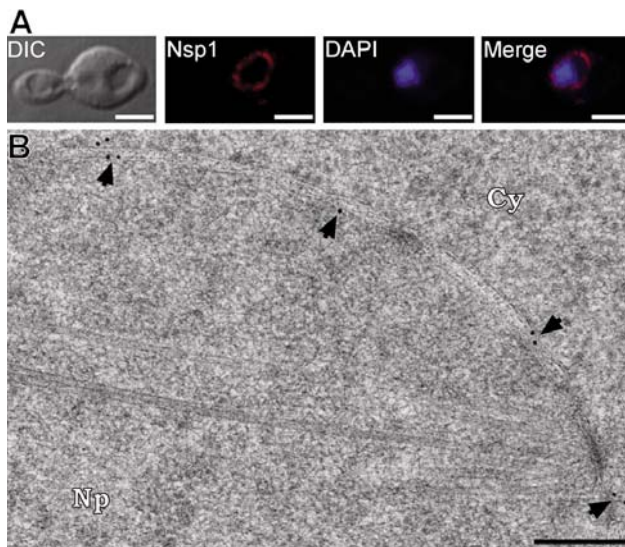


**Fig. 7.** Comparative LM and EM mapping of Nsp1 in *S. cerevisiae* cells. A – DIC, indirect immunofluorescent localization of the nuclear envelope marker protein Nsp1 (red), nuclear DNA staining with DAPI (blue), and their merge. The primary antibody was visualized with a Cy3-conjugated secondary antibody. B – post-embedding on-section immunogold (12 nm) labelling of Nsp1 at the EM level. Gold particles decorate the nuclear pores in the nuclear envelope or are localized in their close proximity (arrowheads). Cy, cytoplasm; Np, nucleoplasm. *S. cerevisiae* cells were freeze-substituted in acetone with 0.1% UA and embedded in Lowicryl HM20. Sections were not post-stained. Scale bar = 3  $\mu$ m (A), 200 nm (B).

et al., 2003). The intensity of the labelling was similar on both chemically fixed and HP-frozen/FS yeast cell sections, though in the case of chemically fixed cells microtubules were not directly visible (data not shown).

## Discussion

In this study, we aimed to find optimal conditions for immunodetection of selected nuclear and nucleolar antigens in *S. cerevisiae* cells both at the LM and EM levels. The fine ultrastructural preservation and the efficiency of the IEM detection was compared on thin sections of cells prepared either by conventional fixation methods at RT or by HPF methods followed by dehydration, infiltration and embedding performed at low (subzero) temperatures.

Chemical fixation was done using either 4% FA (Fig. 1A) or combined FA/GA fixation (Fig. 1B-D), followed by multiple centrifugation, washing and resuspension steps, including sodium metaperiodate and ammonium chloride treatment and LR White embedding (Wright, 2000; Mulholland and Botstein, 2002). Using these processing methods, the majority of the cells showed similar structural preservation and artifacts referred to as “typical” for that kind of processing (see Results). These cells can be used for routine morphological observations, but in most cases they are not suitable for

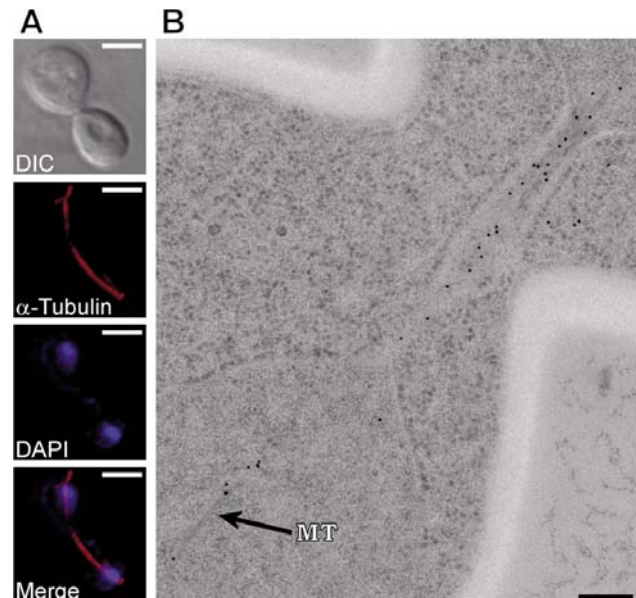


**Fig. 8.** Immunolocalization of  $\alpha$ -tubulin in *S. cerevisiae* cells. Yeast cells in late stages of mitosis are shown. A – DIC, indirect immunofluorescent localization of  $\alpha$ -tubulin (red), nuclear DNA staining with DAPI (blue), and their merge. The primary antibody was visualized with a Cy3-conjugated secondary antibody. Staining revealed both the intranuclear and cytoplasmic microtubules running from the spindle pole bodies embedded in the nuclear envelope. B – post-embedding on-section immunogold (12 nm) labelling of  $\alpha$ -tubulin at the EM level. Microtubules connecting the separated nuclei are specifically labelled (arrow). Mt, microtubule. *S. cerevisiae* cells were freeze-substituted in acetone with 0.1% UA and embedded in Lowicryl HM20. Sections were not post-stained. Scale bar = 3  $\mu$ m (A), 200 nm (B).

immunolocalization experiments due to improper preservation of both the fine ultrastructure and antigenicity. The use of even very weak chemical fixation can destroy some sensitive antigens. In our study, this was the case of Nsr1 and Nsp1, which were successfully localized only in the HP-frozen/FS yeast cells.

An alternative to chemical fixation of the samples is physical fixation, by vitrification, as performed by the HPF method (Dubochet, 2007; McDonald et al., 2007; Studer et al., 2008). It is well known that the specimen loading into the HP-freezer is one of the most critical steps for obtaining well-preserved samples (McDonald, 1999). Concentrating *S. cerevisiae* cells using a vacuum filtration apparatus (McDonald, 2007; Murray, 2008), also used in our experiments (see Material and Methods), proved to be superior to other procedures such as centrifugation or aspiration of the yeast cells into the specimen tubes (Hohenberg et al., 1994). Using this approach it was not necessary to use additive cryo-protectants (e.g. BSA solution, 1-hexadecane, etc.) to achieve flawless cryo-fixation as the homogeneous yeast paste obtained by filtration entirely filled the cavity in the specimen carriers. Immediately after the freezing step, the specimens were dehydrated at low temperatures by

the FS procedure (Schwarz et al., 1993). The details of the FS procedure are generally adapted for the type of material being investigated and for the main goal of the experiment, particularly fine ultrastructural or immunological studies. Different FS protocols for immunocytochemical studies of yeast cells have been published (e.g. Chial et al., 1998; Hofmann et al., 1998; Giddings, 2003; Müller-Reichert et al., 2003). In our protocol we selected the substitution parameters of 24 h at  $-90\text{ }^{\circ}\text{C}$  and 24 h at  $-50\text{ }^{\circ}\text{C}$  in four different FS media (see Material and Methods and Results). To avoid the high temperatures necessary for LR White embedding, we have opted for lowicryl resins designed for low-temperature embedding (Carlemalm et al., 1982). We preferred the non-polar Lowicryl HM20, which was previously successfully used for immunocytochemical studies (Hofmann et al., 1998; Giddings, 2003; Müller-Reichert et al., 2003) despite its hydrophobic properties. The hydrophilic Lowicryls K4M and HM23 were also reported as convenient embedding media (Quintana, 1994; Hofmann et al., 1998).

The cells substituted in acetone alone (Fig. 2A) or in acetone with 0.1% GA (Fig. 2B) showed similar structural preservation. In both cases, however, post-staining was necessary to reveal all the structural features typical of yeast cells. Several previous studies have described FS with acetone only as an approach that often gives unsatisfactory results (Porta and Lopez-Iglesias, 1998), but in others well-preserved samples were obtained (von Schack and Fakan, 1993; Hawes et al., 2007). In our experiments, this procedure resulted in very good overall ultrastructural preservation. The only drawback was the already mentioned detachment of the cells from the resin during the preparation of thin sections. This is often attributed to imperfect infiltration. As described previously (Murray, 2008), it is rather difficult to infiltrate yeast cells with lowicryls at low temperatures. Artifacts such as rupture of the cell wall and even rupture of the nuclear envelope can sometimes be observed. In our experiments, the ultrastructural preservation of the interior of the cells substituted in acetone alone was well preserved without the artifacts mentioned above. However, complete detachment of these cells from the sections occurred frequently, similar to what was observed with LR White-embedded, chemically fixed yeast cells that were not treated with sodium metaperiodate (data not shown). We tried to solve this problem by replacing the acetone/lowicryl mixtures during infiltration by ethanol/lowicryl solutions, since this was suggested to improve infiltration in tissues (Yanick Schwab – personal communication). However, the results were not significantly better (data not shown).

The presence of GA and/or UA in the FS media resulted in the elimination of cell detachments from the lowicryl sections and at the same time improved the preservation of the structure of the cell walls – their fine details became clearly visible in a great majority of cells (Fig. 3A, B). Interestingly, the use of GA as a fixative in the FS media has previously been questioned in some studies, as the addition of aqueous GA increases the wa-

ter content in the substitution mixture and decreases the quality of the ultrastructural preservation (Steinbrecht, 1987). It was shown later that the addition of GA could be profitable (Giddings, 2003). As GA starts to be chemically active only above  $-50\text{ }^{\circ}\text{C}$ , the fixative can infiltrate the whole specimen during the first step of substitution (performed at  $-90\text{ }^{\circ}\text{C}$ ) without reacting (Schwarz et al., 1993). Moreover, the addition of water up to 5 % was shown to markedly enhance membrane contrast without impairing ultrastructural preservation (Walther and Ziegler, 2002). In our experiments, cells substituted in the presence of GA were well preserved (Fig. 2B, 2D and 3A), though occasionally the vacuolar content could be seen to be partially emptied into the cytosol. This phenomenon was also frequently observed in cells substituted in higher concentrations of GA (up to 0.7%) and in acetone/UA/GA-substituted cells (data not shown). Since it was not generally observed in acetone/UA-substituted cells, it may presumably not originate from the high-pressure shock applied during freezing. It is also not obvious to attribute its origin to the action of GA. To our knowledge, this “artifact” has never been described in the literature.

In cells where UA was added to the FS medium, no post-staining was necessary as the UA present produced sufficient contrast (e.g. Figs. 2C, 2D, 3A-F, 4A-D). The cells showed excellent ultrastructural preservation, which makes this type of specimen preparation very convenient for both immunocytochemical and morphological studies. Moreover, since the stain (UA) is distributed throughout the entire volume of the sample and not only at or in the vicinity of the surface as after post-staining, this type of preparation is optimal for electron tomography. On the other hand, because the image is a projection of the section volume onto a plane, the spatial distribution of the stain can blur the details of structures with complex three-dimensional structural organization. This is probably the reason for the improved appearance of the SPB in post-stained samples (Fig. 4E).

### *S. cerevisiae* nuclear ultrastructure

Application of conventional chemical fixation methods that allowed subsequent immunolocalization resulted in nuclei with noticeably irregular shapes in both FA (Fig. 1A) and FA/GA-fixed (Fig. 1B-D) *S. cerevisiae* cells. The nucleoplasm appeared homogeneous without convincing contrast between the regions of heterochromatin and euchromatin.

In HP-frozen/FS *S. cerevisiae* cells, regular and smooth profiles of the nuclei were always observed (Fig. 2A-D). It is known that well-preserved nuclei are the first indication of high-quality cryo-fixation. If the freezing step is not performed adequately, a net-like pattern within the chromatin is often observed, referred to as ice crystal damage (Murray, 2008). In our samples, the material in the nuclei was well-preserved, and very dense. Generally, no reticulation of the chromatin was observed (Fig. 5A-D). The nucleoplasm pattern was almost identical in the cells substituted in all four types of FS media

described above. As reported earlier (von Schack et al., 1991), in cryo-fixed samples of higher eukaryotic cells (not substituted in osmium-acetone mixtures) the chromatin contrast can be "altered" depending on the embedding medium that is used. For example, in acetone alone FS samples embedded in Epon or Lowicryl HM23, the heterochromatin regions were more electron-dense than the euchromatin regions. However, this contrast was reversed when e.g. Lowicryl K11M or LR White was used. In our experiments, the contrast between heterochromatin and euchromatin was visibly improved in HPF/FS samples compared to that observed in the chemically fixed cells, but it still remained rather weak. Neither addition of UA to the FS media (Fig. 5C, D) nor additional post-staining of acetone/UA-substituted cells (data not shown) led to any improvement. Combined with the particular ultrastructure of the yeast nucleoplasm, the identification of the heterochromatin/euchromatin regions was rather difficult. There were, however, some indications suggesting that contrast reversal occurred. More electron-dense chromatin was clearly observed in the nuclear pore areas (Fig. 4A and B, arrowheads), which are generally considered to be devoid of heterochromatin (Fedorova and Zink, 2008).

### *S. cerevisiae* nucleolar ultrastructure

Although the nucleolus of yeast cells is rather well visible at the EM level in most samples prepared by chemical fixation, it is more difficult to distinguish the three distinct nucleolar subcompartments (Melese and Xue, 1995; Sicard et al., 1998; Leger-Silvestre et al., 1999; Trumtel et al., 2000). Unambiguous identification of electron-lucid zones resembling the FCs, surrounded by DFCs and GCs, has been reported only for *S. cerevisiae* cells prepared by cryo-methods (Leger-Silvestre et al., 1999). This identification was questioned, however (Thiry and Lafontaine, 2005), and it was proposed that *S. cerevisiae* nucleoli exhibit bipartite organization as only FC and GC compartments could be unambiguously discerned.

In our experiments, most of the investigated nucleoli in FA and FA/GA-fixed *S. cerevisiae* cells had barely detectable subnucleolar organization (Fig. 1A-D). Electron-lucid zones surrounded by zones of higher electron densities were occasionally observed, although the pre-ribosomal particles that are known to form the GCs were not seen clearly. In contrast, the nucleoli of HP-frozen yeast cells showed detailed nucleolar ultrastructure in all four types of FS media that were used (Fig. 5A-D). The electron-lucid FCs could be clearly distinguished (Fig. 5, asterisks) against the dense chromatin that formed the rest of the nucleolus and exhibited both granular and fibrillar aspects (Fig. 5, arrowheads). Thus it was hard to identify the electron-dense areas as either DFCs or GCs, though they are predicted to have different ultrastructural arrangements. Out of all four FS media, the nucleoli of acetone/UA-substituted yeast cells were the most distinct with slightly coarser structure (Fig. 5B). Since clear FC/DFC/GC compartmentalization was never ob-

served in any of our samples, our findings are in agreement with the bipartite model of *S. cerevisiae* nucleolar organization (Thiry and Lafontaine, 2005).

### Immunocytochemistry

Different proteins closely associated with nuclear (Nsp1) or nucleolar (Nop1 and Nsr1) functions as well as  $\alpha$ -tubulin were selected as target antigens for both LM and EM detection. Immunocytochemical studies performed on thin sections of cells prepared with our HPF/FS protocol gave very satisfactory results, often revealing antigenic sites which were hardly or not at all detected in cells processed by conventional chemical fixation procedures. Thanks to the improved ultrastructural preservation it was much easier to simultaneously correlate the localization of specific antigenic sites with fine details preserved in the cell nucleus. Thus, Nop1 (Fig. 6B) and Nsr1 (Fig. 6D) were clearly localized to the dense parts of the yeast nucleolus, mostly resembling the DFCs. Interestingly, no Nsr1 labelling was detected on sections of both FA and FA/GA-fixed yeast cells. A similar situation was observed in the case of Nsp1, which was otherwise clearly detected on sections of HP-frozen/FS cells (Fig. 7B). To determine whether the antigenicity of these proteins was impaired by the fixation procedure or by heat polymerization (+47 °C in the case of LR White), the HP-frozen/FS yeast cells were embedded in LR White. Both antigens gave the same pattern and labelling intensity as in Lowicryl HM20 low-temperature embedded samples (data not shown), thus demonstrating that in this particular case the chemical fixation, despite being very weak, was probably the main cause of antigenicity loss, and not the heat polymerization. The pattern of  $\alpha$ -tubulin labelling was the same in both HP-frozen/FS (Fig. 8B) and FA and FA/GA-fixed yeast cells (data not shown).

Next, we compared the efficiency of on-section immunogold labelling of Nop1 and Nsr1 antigens between yeast cells substituted in the different FS media described in this study. With the exception of acetone/GA, the immunolabelling efficiency revealed to be approximately equal (within the error bar) for all used FS media, giving for the nucleolus area approximately 23 and 16 gold particles/ $\mu\text{m}^2$  for Nop1 and Nsr1, respectively. On the other hand, the non-specific background labelling (outside the nucleolus) was increased in acetone-only and acetone/GA FS samples,  $2 \pm 5$  gold particles/ $\mu\text{m}^2$  for Nop1 and  $4 \pm 5$  for Nsr1, while in other two media it was below 0.5 for both antibodies. This would suggest a positive role of UA in suppression of non-specific labelling. Similar results with increasing non-specific labelling were previously observed in cryo-fixed/FS tissue samples (von Schack and Fakan, 1993) and in HP-frozen and subsequently rehydrated samples (van Donselaar et al., 2007). Although efficient immunodetection of particular antigens was reported even after adding GA to FS media at a concentration of up to 0.25 % (McDonald and Müller-Reichert, 2002; Giddings, 2003; Hawes et al., 2007), we decided to keep the

concentrations of both GA and UA very low (0.1 % final) in the present study in order to maximize retention of antigenicity for the tested antigens. Even at this concentration, the addition of GA to acetone had an opposite effect on the localization of the two antigens. While for Nop1 the intensity of labelling doubled to  $50 \pm 12$  gold particles/ $\mu\text{m}^2$ , in the case of Nsr1 it dropped to  $8 \pm 2$  gold particles/ $\mu\text{m}^2$ . This suggests that use of GA as the only fixative in the substitution media can have an unpredictable impact on the immunolabelling efficiency. The addition of UA or combination of GA with UA to FS media therefore seems to be a more recommendable choice.

In conclusion, we have compared in this study different ways to prepare *S. cerevisiae* cells for immunolocalization of proteins known to be closely related to nuclear and nucleolar functions, both at the LM and EM levels. An approach using weak chemical fixation was compared with a high-pressure freezing method followed by dehydration via freeze-substitution in different substitution media. Out of all tested combinations, we found the freeze-substitution in acetone with 0.1% UA and low-temperature embedding in Lowicryl HM20 to be the most universal and to give the best preserved *S. cerevisiae* cells for both morphological and immunological studies.

### Acknowledgements

We are grateful to Yvonne S. Osheim and Ann L. Beyer from the Department of Microbiology, University of Virginia Health System (Charlottesville, VA), for providing the yeast cell strain NOY 886. We also thank Lubomír Kováčik for assistance with the preparation of figures and Christian Lanctôt and Guy Hagen for critical editing of the manuscript.

### References

- Bailer, S. M., Balduf, C., Hurt, E. (2001) The Nsp1p carboxy-terminal domain is organized into functionally distinct coiled-coil regions required for assembly of nucleoporin subcomplexes and nucleocytoplasmic transport. *Mol. Cell. Biol.* **21**, 7944-7955.
- Bendayan, M., Shore, G. C. (1982) Immunocytochemical localization of mitochondrial proteins in the rat hepatocyte. *J. Histochem. Cytochem.* **30**, 139-147.
- Buser, C., Walther, P. (2008) Freeze-substitution: the addition of water to polar solvents enhances the retention of structure and acts at temperatures around -60 degrees C. *J. Microsc.* **230**, 268-277.
- Carlemalm, E., Garavito, R. M., Villiger, W. (1982) Resin development for electron-microscopy and an analysis of embedding at low-temperature. *J. Microsc.* **126**, 123-143.
- Chial, H. J., Rout, M. P., Giddings, T. H., Winey, M. (1998) *Saccharomyces cerevisiae* Ndc1p is a shared component of nuclear pore complexes and spindle pole bodies. *J. Cell Biol.* **143**, 1789-1800.
- Derenzini, M., Montanaro, L., Trere, D. (2009) What the nucleolus says to a tumour pathologist. *Histopathology* **54**, 753-762.
- Dubochet, J. (2007) The physics of rapid cooling and its implications for cryoimmobilization of cells. *Methods Cell Biol.* **79**, 7-21.
- Escande, M. L., Gas, N., Stevens, B. J. (1985) Immunolocalization of the 100 K nucleolar protein in CHO cells. *Biol. Cell* **53**, 99-109.
- Fahrenkrog, B., Aris, J. P., Hurt, E. C., Pante, N., Aebi, U. (2000) Comparative spatial localization of protein-A-tagged and authentic yeast nuclear pore complex proteins by immunogold electron microscopy. *J. Struct. Biol.* **129**, 295-305.
- Fedorova, E., Zink, D. (2008) Nuclear architecture and gene regulation. *Biochim. Biophys. Acta* **1783**, 2174-2184.
- Giddings, T. H. (2003) Freeze-substitution protocols for improved visualization of membranes in high-pressure frozen samples. *J. Microsc.* **212**, 53-61.
- Griffith, J., Mari, M., De Maziere, A., Reggiori, F. (2008) A cryosectioning procedure for the ultrastructural analysis and the immunogold labelling of yeast *Saccharomyces cerevisiae*. *Traffic* **9**, 1060-1072.
- Gulli, M. P., Girard, J. P., Zabetakis, D., Lapeyre, B., Melese, T., Caizergues-Ferrer, M. (1995) gar2 is a nucleolar protein from *Schizosaccharomyces pombe* required for 18S rRNA and 40S ribosomal subunit accumulation. *Nucleic Acids Res.* **23**, 1912-1918.
- Hawes, P., Netherton, C. L., Mueller, M., Wileman, T., Monaghan, P. (2007) Rapid freeze-substitution preserves membranes in high-pressure frozen tissue culture cells. *J. Microsc.* **226**, 182-189.
- Hernandez-Verdun, D. (2006) The nucleolus: a model for the organization of nuclear functions. *Histochem. Cell Biol.* **126**, 135-148.
- Hofmann, C., Cheeseman, I. M., Goode, B. L., McDonald, K. L., Barnes, G., Drubin, D. G. (1998) *Saccharomyces cerevisiae* Duo1p and Dam1p, novel proteins involved in mitotic spindle function. *J. Cell Biol.* **143**, 1029-1040.
- Hohenberg, H., Mannweiler, K., Muller, M. (1994) High-pressure freezing of cell suspensions in cellulose capillary tubes. *J. Microsc.* **175**, 34-43.
- Humbel, B. M., Konomi, M., Takagi, T., Kamasawa, N., Ishijima, S. A., Osumi, M. (2001) In situ localization of beta-glucans in the cell wall of *Schizosaccharomyces pombe*. *Yeast* **18**, 433-444.
- Kilmartin, J. V., Adams, A. E. (1984) Structural rearrangements of tubulin and actin during the cell cycle of the yeast *Saccharomyces*. *J. Cell Biol.* **98**, 922-933.
- Kondo, K., Inouye, M. (1992) Yeast NSR1 protein that has structural similarity to mammalian nucleolin is involved in pre-rRNA processing. *J. Biol. Chem.* **267**, 16252-16258.
- Lee, W. C., Zabetakis, D., Melese, T. (1992) NSR1 is required for pre-rRNA processing and for the proper maintenance of steady-state levels of ribosomal subunits. *Mol. Cell. Biol.* **12**, 3865-3871.
- Leger-Silvestre, I., Gulli, M. P., Noaillac-Depeyre, J., Faubladiere, M., Sicard, H., Caizergues-Ferrer, M., Gas, N. (1997) Ultrastructural changes in the *Schizosaccharomyces pombe* nucleolus following the disruption of the gar2+ gene, which encodes a nucleolar protein structurally related to nucleolin. *Chromosoma* **105**, 542-552.
- Leger-Silvestre, I., Trumtel, S., Noaillac-Depeyre, J., Gas, N. (1999) Functional compartmentalization of the nucleus in

- the budding yeast *Saccharomyces cerevisiae*. *Chromosoma* **108**, 103-113.
- McDonald, K. (1999) High-pressure freezing for preservation of high resolution fine structure and antigenicity for immunolabeling. *Methods Mol. Biol.* **117**, 77-97.
- McDonald, K., Muller-Reichert, T. (2002) Cryomethods for thin section electron microscopy. *Methods Enzymol.* **351**, 96-123.
- McDonald, K. (2007) Cryopreparation methods for electron microscopy of selected model systems. *Methods Cell Biol.* **79**, 23-56.
- McDonald, K. L., Morphew, M., Verkade, P., Muller-Reichert, T. (2007) Recent advances in high-pressure freezing: equipment- and specimen-loading methods. *Methods Mol. Biol.* **369**, 143-173.
- Melese, T., Xue, Z. (1995) The nucleolus: an organelle formed by the act of building a ribosome. *Curr. Opin. Cell Biol.* **7**, 319-324.
- Mosgoeller, W. (2004) Nucleolar ultrastructure in vertebrates. In: *The Nucleolus*, ed. Olson, M. O. J., pp 10-20, Eurekah.com and Kluwer Academic, New York, USA.
- Mulholland, J., Botstein, D. (2002) Immunoelectron microscopy of aldehyde-fixed yeast cells. *Methods Enzymol.* **351**, 50-81.
- Müller-Reichert, T., Sassoon, I., O'Toole, E., Romao, M., Ashford, A. J., Hyman, A. A., Antony, C. (2003) Analysis of the distribution of the kinetochore protein Ndc10p in *Saccharomyces cerevisiae* using 3-D modeling of mitotic spindles. *Chromosoma* **111**, 417-428.
- Murray, S. (2008) High pressure freezing and freeze substitution of *Schizosaccharomyces pombe* and *Saccharomyces cerevisiae* for TEM. *Methods Cell Biol.* **88**, 3-17.
- Porta, D., Lopez-Iglesias, C. (1998) A comparison of cryo-versus chemical fixation in the soil green algae *Jaagielia*. *Tissue Cell* **30**, 368-376.
- Pringle, J. R., Preston, R. A., Adams, A. E., Stearns, T., Drubin, D. G., Haarer, B. K., Jones, E. W. (1989) Fluorescence microscopy methods for yeast. *Methods Cell Biol.* **31**, 357-435.
- Qiu, H., Eifert, J., Wacheul, L., Thiry, M., Berger, A. C., Jakovljevic, J., Woolford, J. L., Jr., Corbett, A. H., Lafontaine, D. L., Terns, R. M., Terns, M. P. (2008) Identification of genes that function in the biogenesis and localization of small nucleolar RNAs in *Saccharomyces cerevisiae*. *Mol. Cell. Biol.* **28**, 3686-3699.
- Quintana, C. (1994) Cryofixation, cryosubstitution, cryoembedding for ultrastructural, immunocytochemical and micro-analytical studies. *Micron* **25**, 63-99.
- Reynolds, E. S. (1963) The use of lead citrate at high pH as an electron-opaque stain in electron microscopy. *J. Cell Biol.* **17**, 208-212.
- Sato, M., Kobori, H., Ishijima, S. A., Feng, Z. H., Hamada, K., Shimada, S., Osumi, M. (1996) *Schizosaccharomyces pombe* is more sensitive to pressure stress than *Saccharomyces cerevisiae*. *Cell Struct. Funct.* **21**, 167-174.
- Schimmang, T., Tollervey, D., Kern, H., Frank, R., Hurt, E. C. (1989) A yeast nucleolar protein related to mammalian fibrillarin is associated with small nucleolar RNA and is essential for viability. *EMBO J.* **8**, 4015-4024.
- Schwarz, H. Hohenberg, H., Humbel, B. M. (1993) Freeze-substitution in virus research: a preview. In: *Immuno-gold Electron Microscopy in Virus Diagnosis and Research*, eds. Hyatt A. D., Eaton, B. T., pp. 349-376, CRC Press, Inc., Boca Raton, Florida, USA.
- Shaw, P., Doonan, J. (2005) The nucleolus. Playing by different rules? *Cell Cycle* **4**, 102-105.
- Sicard, H., Faubladiere, M., Noaillac-Depeyre, J., Leger-Silvestre, I., Gas, N., Caizergues-Ferrer, M. (1998) The role of the *Schizosaccharomyces pombe* gar2 protein in nucleolar structure and function depends on the concerted action of its highly charged N terminus and its RNA-binding domains. *Mol. Biol. Cell.* **9**, 2011-2023.
- Sirri, V., Urcuqui-Inchima, S., Roussel, P., Hernandez-Verdun, D. (2008) Nucleolus: the fascinating nuclear body. *Histochem. Cell Biol.* **129**, 13-31.
- Spector, D. L., Ochs, R. L., Busch, H. (1984) Silver staining, immunofluorescence, and immunoelectron microscopic localization of nucleolar phosphoproteins B23 and C23. *Chromosoma* **90**, 139-148.
- Studer, D., Humbel, B. M., Chiquet, M. (2008) Electron microscopy of high pressure frozen samples: bridging the gap between cellular ultrastructure and atomic resolution. *Histochem. Cell Biol.* **130**, 877-889.
- Thiry, M., Lafontaine, D. L. (2005) Birth of a nucleolus: the evolution of nucleolar compartments. *Trends Cell Biol.* **15**, 194-199.
- Tollervey, D., Lehtonen, H., Carmo-Fonseca, M., Hurt, E. C. (1991) The small nucleolar RNP protein NOP1 (fibrillarin) is required for pre-rRNA processing in yeast. *EMBO J.* **10**, 573-583.
- Trumtel, S., Leger-Silvestre, I., Gleizes, P. E., Teulieres, F., Gas, N. (2000) Assembly and functional organization of the nucleolus: ultrastructural analysis of *Saccharomyces cerevisiae* mutants. *Mol. Biol. Cell* **11**, 2175-2189.
- van Donselaar, E., Posthuma, G., Zeuschner, D., Humbel, B. M., Slot, J. W. (2007) Immunogold labeling of cryosections from high-pressure frozen cells. *Traffic* **8**, 471-485.
- van Tuinen, E., Riezman, H. (1987) Immunolocalization of glyceraldehyde-3-phosphate dehydrogenase, hexokinase, and carboxypeptidase Y in yeast cells at the ultrastructural level. *J. Histochem. Cytochem.* **35**, 327-333.
- Vanhecke, D., Graber, W., Studer, D. (2008) Close-to-native ultrastructural preservation by high pressure freezing. *Methods Cell Biol.* **88**, 151-164.
- von Schack, M. L., Fakan, S., Villiger, W. (1991) Some applications of cryosubstitution in ultrastructural studies of the cell nucleus. *Biol. Cell* **72**, 113-119.
- von Schack, M. L., Fakan, S. (1993) The study of the cell nucleus using cryofixation and cryosubstitution. *Micron* **24**, 507-519.
- Walther, P., Ziegler, A. (2002) Freeze substitution of high-pressure frozen samples: the visibility of biological membranes is improved when the substitution medium contains water. *J. Microsc.* **208**, 3-10.
- Wright, R. (2000) Transmission electron microscopy of yeast. *Microsc. Res. Tech.* **51**, 496-510.
- Xu, C., Henry, P. A., Setya, A., Henry, M. F. (2003) In vivo analysis of nucleolar proteins modified by the yeast arginine methyltransferase Hmt1/Rmt1p. *RNA* **9**, 746-759.
- Yan, C., Melese, T. (1993) Multiple regions of NSR1 are sufficient for accumulation of a fusion protein within the nucleolus. *J. Cell Biol.* **123**, 1081-1091.